Environment International 121 (2018) 1113–1120

Contents lists available at ScienceDirect

Environment International

journal homepage: www.elsevier.com/locate/envint

Release and toxicity of adipose tissue-stored TCDD: Direct evidence from a xenografted fat model

Nolwenn Joffin[a,b,j,1], Philippe Noirez[a,b,c,d,e,j,1], Jean-Philippe Antignac[g], Min-ji Kim[a,f], Philippe Marchand[g], Marion Falabregue[b,c,d,j], Bruno Le Bizec[g], Claude Forest[a,b,j], Claude Emond[e,h,i], Robert Barouki[a,b,j,*], Xavier Coumoul[a,b,j,*]

[a] INSERM UMR-S1124, Toxicologie Pharmacologie et Signalisation cellulaire, France
[b] Université Paris Descartes, 45 rue des Saints-Pères, 75006 Paris, France
[c] IRMES, EA 7329, Institut de Recherche bioMédicale et d'Epidémiologie du Sport, Paris, France
[d] Institut National du Sport, de l'Expertise et de la Performance (INSEP), Paris, France
[e] Université du Québec à Montréal (UQAM), Montreal, Qc, Canada
[f] Université Paris 13, Sorbonne Paris Cité, Bobigny, France
[g] Laboratoire d'Etude des Résidus et Contaminants dans les Aliments (LABERCA), UMR 1329 Oniris-INRA, Nantes, France
[h] BioSimulation Consulting Inc., Newark, DE 19713, USA
[i] Université de Montréal, Montreal, Qc, Canada
[j] Sorbonne Paris Cité, Paris, France

ARTICLE INFO

Handling Editor: Heather Stapleton

Keywords:
Adipose tissue
Graft
Internal release
Dioxin
TCDD
PBPK
Fibrosis

ABSTRACT

Background: Persistent organic pollutants (POPs) are known to accumulate in adipose tissues (AT). This storage may be beneficial by diverting POPs from other sensitive tissues or detrimental because of chronic release of pollutants as indirectly suggested during weight loss. The aim is to study the biological and/or toxic effects that chronic POP release from previously contaminated grafted AT could exert in a naïve mouse.

Methods: C57BL/6J male mice were exposed intraperitoneally to 2,3,7,8-tetrachlorodibenzo-*p*-doxin (TCDD); their epididymal fat pads were collected and grafted on the back skin of uncontaminated recipient mice whose brain, liver, and epididymal ATs were analyzed (TCDD concentration, relevant gene expression). Kinetics of release and redistribution were modeled using Physiologically Based PharmacoKinetics (PBPK).

Results: The grafts released TCDD over a period of 10 weeks with different kinetics of distribution in the three organs studied. A PBPK model was used to simulate the AT releasing process and the incorporation of TCDD into the major organs. At three weeks post-graft, we observed significant changes in gene expression in the liver and the host AT with signatures reminiscent of inflammation, gluconeogenesis and fibrosis as compared to the control.

Conclusions: This study confirms that AT-stored TCDD can be released and distributed to the organs of the recipient hence leading to distinct changes in gene expression. This original model provides direct evidence of the potential toxic-relevant effects when endogenous sources of contamination are present.

List of abbreviations: alpha-SMA, alpha-smooth muscle actin; AhR, aryl hydrocarbon receptor; AQP, aquaporin; AT, adipose tissue; ATGL, adipose triglyceride lipase; bw, body weight; CD, cluster of differentiation; COL1A1, collagen 1A1; CPT1B, carnitine palmitoyl-transferase 1B; CYP, cytochrome P450; FABP4, fatty acid binding protein 4; FAS, fatty acid synthase; G6Pase, glucose-6 phosphatase; HSL, hormone-sensitive lipase; IL, interleukin; MCP-1, monocyte chemoattractant protein-1; NOS2, NO synthase 2; PAI-1, plasminogen activator inhibitor-1; PBPK, physiologically based pharmacokinetic; PC, pyruvate carboxylase; PCB, polychlorinated biphenyl; PDK, pyruvate dehydrogenase kinase; PEPCK, phosphoenolpyruvate carboxykinase; PGC-1 alpha, PPARg-coactivator 1 alpha; POPs, persistent organic pollutants; PPARα, peroxisome proliferator-activated receptor-alpha; PPARg2, PPAR-gamma2; RT-qPCR, real-time quantitative PCR; SD, standard deviation; TNF, tumor-necrosis factor; UCP1, uncoupling protein 1; VLCAD, very long-chain acyl-CoA dehydrogenase; PBPK, Physiologically Based PharmacoKinetic

* Corresponding authors at: INSERM UMR-S1124, Toxicologie Pharmacologie et Signalisation cellulaire, France.
E-mail addresses: robert.barouki@parisdescartes.fr (R. Barouki), xavier.coumoul@parisdescartes.fr (X. Coumoul).
[1] Equal contributions.

https://doi.org/10.1016/j.envint.2018.10.027
Received 28 June 2018; Received in revised form 12 October 2018; Accepted 14 October 2018
Available online 31 October 2018

1. Introduction

Persistent organic pollutants (POPs) are xenobiotics of major concern for environmental health (Bonde et al., 2016; Mostafalou, 2016; Smarr et al., 2016). 2,3,7,8-Tetrachlorodibenzo-*p*-dioxin (TCDD) is one of the most potent compounds among the dioxin class of substances and its toxicity equivalence factor is set to a reference value of 1. TCDD binds to the Aryl hydrocarbon Receptor (AhR), a protein of the basic Helix-Loop-Helix/Per – ARNT – Sim (bHLH/PAS) family, which transcriptionally activates the expression of genes which code for xenobiotic metabolizing enzymes (XME) as well as that of other genes (Guyot et al., 2013). However, in spite of the induction of these detoxifying enzymes, the TCDD and other POPs are very poorly metabolized and, therefore, not readily eliminated. This, as well as their lipophilicity, accounts for their accumulation in adipose tissue (AT) (Lee et al., 2017).

The storage of POPs in AT is believed to have complex implications and consequences (Kim et al., 2011, 2012). It may be protective to a certain extent since it diverts POPs from critical target organs such as the brain. However, it is also assumed that contaminated AT progressively delivers POPs that would eventually lead to a chronic low-rating release resulting in chronic toxicity. Indeed, we and others observed an increase in blood POPs following weight loss (Chevrier et al., 2000; Imbeault et al., 2002; Kim et al., 2011) but such increase could also be the result of the dynamic switch between lipolysis and lipogenesis that occurs during fasting/feeding process, independent of weight loss. The evidence for both scenarios, i.e. protection and long-term toxicity, is indirect at this stage.

Long-term exposure to TCDD has been associated with many pathologies including cancer, infertility or metabolic diseases (White and Birnbaum, 2009). Its carcinogenic effects have been established by the World Health Organization (WHO) and the US National Toxicology Program (NTP) despite some conflicting results in humans (Boffetta et al., 2011). Regarding metabolic diseases, a recent meta-analysis pointed to a likely link between TCDD exposure and type 2 diabetes (Goodman et al., 2015), while in vitro and in vivo experiments showed that TCDD reduced glucose uptake by the liver and AT, a process that occurs with decreases in insulin production and secretion by beta-pancreatic cells (Novelli et al., 2005). TCDD is also suspected to elicit metabolic diseases through either the induction of local inflammation of the AT (Kim et al., 2012), the regulation of endogenous metabolizing enzymes (carbohydrate and lipid pathways) (Ambolet-Camoit et al., 2015) or epigenetic mechanisms. Such TCDD effects are consistent with the suspected obesogen effects of several POPs (i.e. organochlorinated pesticides) (La Merrill et al., 2013; Lee et al., 2016).

While the long-term toxicity of TCDD (and other POPs) is now established, there is still no direct evidence that its release from AT is involved in such long-term toxicity although such effects are being suspected (Kim et al., 2011). In all experimental protocols, animals are either fed or injected with TCDD, resulting in single (or repetitive) exposures. There are several possible mechanisms for long-term toxicity. Such toxicity may be due to the direct effect of ingested TCDD following exposure but could also be additionally due to TCDD output from internal compartments like AT. Because of the lack of an experimental model assessing the role of AT-stored TCDD, it has not been possible yet to assess those hypotheses and to clearly identify the kinetic and dynamic behaviors of TCDD discharged from internal storage sites.

The aims of the present study were 1) to develop an experimental model based on a surgical graft procedure; 2) to describe the fate and effects of AT-stored TCDD then specifically investigate whether this compound can be discharged from the AT and display activity on other tissues, and 3) to build a physiologically based pharmacokinetic (PBPK) model to simulate the distribution of TCDD by gavage and the donor, and then at the second time simulating a chronic endogenous POP release from the graft implant in the host, and 4) to characterize the effects of this release on the expression of several biomarkers linked to pathologies. To achieve this goal, we have developed a unique, new and original experimental model allowing such investigation. We have grafted TCDD-contaminated AT to uncontaminated mice and monitored the action that sub-chronic release of this POP could exert in three host tissues, AT, liver and brain; such novel bioengineered mice allowed the generation of a PBPK model simulating a chronic POP output from a grafted implant. We characterized the effects of this release on the expression of several biomarkers linked to the above-described pathologies - including endogenous metabolic enzymes or inflammatory cytokines - in recipient AT and liver, two organs that are critically involved in metabolic regulations.

2. Materials and methods

2.1. Mice

The European Communities Council Directive 2010/63/EU on the protection of the animals was followed for the experiments using animals. All procedures were approved by the ethical committee for animal research of Paris Descartes university (CEEA.34, number: 12-132). C57BL/6J male mice (12-week-old) with body weight (bw) about 25 g were obtained from Janvier and allowed 1 week to acclimate at the Paris Descartes university animal facility before the study. Animals were maintained on a 12-h light/dark cycle at the ambient temperature of a 22 ± 1 °C and relative humidity of 55 ± 5% and were provided with Purina 5001 rodent Chow (Safe) and tap water ad libitum.

2.2. Primary POPs exposure

The mice donor C57BL/6J received a single intraperitoneal injection with either dose of 0, 1, 10 or 25 µg TCDD/kg of bw in corn oil. Mice were sacrificed 48 h after injection. For each mouse, both epididymal fat pads were collected: one was used for TCDD quantification and the other for the graft to a donor mouse.

2.3. Graft of epididymal AT contaminated with POPs

Each epididymal fat pad was grafted into the subcutaneous plane on the back of the mice. Mice were sacrificed at 0.5, 1, 2, 3, 4 or 10 weeks following the graft. The graft, brain, liver, and epididymal AT were removed for quantification of TCDD and gene analyses. We observed that the grafts were revascularized between 4 and 10 weeks following the surgical procedure (data not shown).

2.4. POPs internal exposure levels quantification

The methodology that was applied to isolate, detect, and quantify TCDD had its origin in a more global previously described method used for measuring dioxins and PCBs (Costera et al., 2006). Briefly, ^{13}C-labelled TCDD was added to each sample for quantification according to the isotopic dilution method. Samples of AT (50 to 250 mg), liver (0.150 to 1.750 g) and brain (150 to 550 mg) were first submitted to an accelerated solvent extraction at high temperature and high pressure (ASE Dionex, Sunnyvale, CA). The resulting extracts were weighed to evaluate fat content by a gravimetric method and were reconstituted in hexane for further sample clean up through three purification steps using successively acid silica, florisil, and celite/carbon columns. TCDD concentrations were assessed using gas chromatography (Agilent 7890A) coupled to high-resolution mass spectrometry (GC-HRMS) on electromagnetic sector instrument (JEOL MS 800D), operating at 10,000 resolutions and in the single ion monitoring (SIM) acquisition mode. This method was validated according to current European criteria in the field of regular control of foodstuff of animal origin and accredited according to the ISO 17025 standard.

2.5. PBPK modeling

Several models have been published to mimic the pharmacokinetics of TCDD on different species (Emond, 2004; Kissel and Robarge, 1998; Leung et al., 1990, 1988). More recently, a PBPK model for TCDD has been applied to humans and mice (Emond et al., 2010; Emond et al., 2016) to study the influence of obesity and diabetes on the elimination of TCDD (Emond et al., 2018). A larger description and assessment work of the PBPK model for mice were performed and peer-reviewed during the NCEA-USEPA reassessment (USEPA, 2012). This version of the PBPK model was used as a base for the present work. Briefly, the model is originally composed of 3 compartments (liver, AT and the rest of the body) connected to the systemic circulation (arterial and venous). The rest of the body compartment is composed of muscles (≈70%) and other non-essential organs for the pharmacokinetics but is required for the mass balance calculation. The rest of the body is then described as permeability-limited compartments (composed of extracellular matrix and blood sub-compartments). The elimination of TCDD from the body is very limited; it happens mostly in the feces and not much in the urine. In addition, the PBPK model also integrates an enterohepatic cycle; overall, it allows the description of an elimination rate based on the body burden using a mathematical component function (Emond et al., 2016; USEPA, 2012). One key parameter of this model, which conditions the elimination rate of TCDD, is the induction of CYP1A2 which is due to AhR activation (CY1A2 is a transcriptional target of the AhR) which depends on the body burden (Diliberto et al., 1997; Emond et al., 2005, 2006). All the parameters used in this PBPK model, before modification, were previously assessed and presented in the USEPA, 2012 report (in this reference, see Tables 3–8 pages 3–63).

To describe the release of TCDD from the AT implanted in the dorsal subcutaneous skin region (graft), it was necessary to update the original PBPK model by adding a skin compartment and graft (Fig. 1).

Indeed, we assumed that the graft was an entity added to the skin compartment. Basically, the graft releases the TCDD which diffuses to the skin compartment and is then released in the blood. The blood flow in the skin compartment was described as permeability-limited; all parameters for this additional compartment including the partition coefficient “skin/blood” (unitless), perfusion of the skin compartment

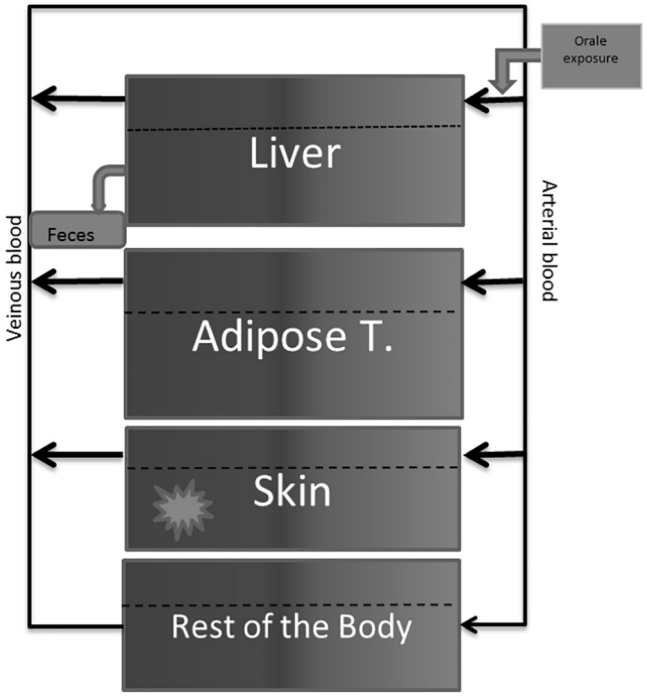

Fig. 1. Conceptual representation of the PBPK model in mice.

Table 1
Physiological parameters used to define both skin and graft compartments used in the PBPK allografted mice model.

Parameters	Name of the parameters	Values	References
V_{sk}	Fraction of body weight for skin (unitless)	0.165	Brown et al., 1997
V_{skb}	Fraction of tissue blood volumes for skin (unitless)	0.0159	Wang et al., 1997
Q_{skf}	Tissue blood flow fraction of cardiac output for skin (unitless)	0.057	Brown et al., 1997
$P_{sk/b}$	Partition coefficient (skin/blood) (unitless)	10	Wang et al., 1997
KGRAFT	First order parameter of TCDD release in graft to the skin (h^{-1})	0.004	Optimized
PASKINF	Diffusion permeability (unitless)	0.09	Optimized
R	Fraction of blood diffusion (PASKIN) from the blood skin to the grafted starting 4 weeks post-graft implantation (unitless)	$R = 0.0007$	Optimized

($mL{\cdot}h^{-1}$), the diffusion permeability of the skin ($mL{\cdot}h^{-1}$) and the volume of skin tissue (mL) were extracted from the literature (Brown et al., 1997; Wang et al., 1997) (Table 1).

The graft sub-compartment is essentially composed of TCDD-delivering AT (see Section 2.2). This delivery was estimated using the concentration of TCDD in the graft at time 0 and the subsequent measurements at different time points (using a first order kinetic release of TCDD from the graft to the skin). We also consider a functional vascularization of the graft around week 4 (visual observation). The parameters used to mimic mathematically the release of TCDD from the graft are presented in Table 2.

The amount of TCDD which remains in the graft after each time point (dt), also agraftresnmol, was estimated using Eq. (1):

- **Equation 1**: Variation of the amount of TCDD (nmole) that remains in the graft after each time interval (dt) in hours

$$\frac{dagrafnmol\,(nmoL)}{dt\,(h)} = -kgraft \times agraftresnmol \tag{1}$$

Then, the changes in TCDD concentrations in the grafts were estimated using Eqs. (2) & (3).

- **Equation 2**: Amount of TCDD (nmoles) remaining in the graft after each time point (dt):

$$agraftresnmol = \int_{t-1}^{t} agraftnmol \tag{2}$$

- **Equation 3**: Concentration of TCDD in pg/g

$$agraftrespgg\left(\frac{pg}{g}\right) = agraftresnmol\,(nmole) \times \frac{MW\left(\frac{ng}{nmole}\right) \times 1000\left(\frac{pg}{ng}\right)}{graftmass\,(g)} \tag{3}$$

Table 2
Parameters used to mimic mathematically the release of TCDD from the graft in the corresponding equations.

Parameters	Description of the parameters
cgraft0	Concentration of TCDD in the graft at time 0 ($pg{\cdot}g^{-1}$)
graftmass	Mass of the graft (g)
agraftpg	Amount of TCDD at time 0 (pg)
kgraft	Constant transfer of TCDD from graft to skin (h^{-1})
agraftng	Amount of TCDD in the graft at time 0 (ng)
agraftnmol	Amount of TCDD in the graft at time 0 (nmole)
agraftresnmol	Amount of TCDD remaining in the graft at different time points (nmole)

These simulation parameters were optimized by a first series of experiments carried out to assess the release of TCDD from the graft during the optimization of the exposure dose of the donor. Determination of the graft mass and the concentration of TCDD at different time points were compared to the simulation profile resulting from the model. In addition, simulation of TCDD generated using the PBPK model was compared to the experimental time points determined experimentally.

2.6. RNA sampling from tissues

AT and liver samples were placed in 1 mL of Qiazol® reagent with 2 stainless steel beads (Qiagen, France) and were homogenized with a TissueLyser system (RetschMM300, Germany). Total RNA was prepared using the RNeasy Mini Kit following the manufacturer's instructions (Qiagen, France). The quality of total RNA was monitored with a Nanodrop ND-1000 spectrophotometer (Nanodrop products, Wilmington, USA).

2.7. Quantitative real-time PCR

Reverse transcription was carried out using the High Capacity cDNA Reverse Transcription Kit (Life technology, France) according to the manufacturer's directions. Real-time PCR was achieved with 20 ng of cDNA, with duplicates for each experiment. STable 1 (Suppl Mat.) gives the gene-specific primers. The relative amounts of mRNA were estimated using the $\Delta\Delta C_T$ method with Ribosomal Protein L13 (RPL13) as the reference gene (Juricek et al., 2014; Pfaffl, 2001).

2.8. Statistical analyses

Unless otherwise specified, two-group and multiple-group comparisons were made using Mann–Whitney's *U* test (nonparametric comparison of two independent series) or Kruskal-Wallis test followed by a pair-wise Dunn's post hoc test (nonparametric comparison of multiple independent series). A *p*-value < 0.05 was considered statistically significant (***$p < 0.001$, **$p < 0.01$; *$p < 0.05$). The values are expressed as the mean ± standard deviation.

3. Results

3.1. Xenografted-adipose tissue releases TCDD

Vehicle (control) or three different doses of TCDD (1, 10 or 25 μg·kg^{-1} bw; corn oil as a control) were intraperitoneally injected to C57BL6/J male mice that were sacrificed 48 h later. TCDD concentration was determined in the epididymal AT of control (corn oil) and exposed mice, showing a proportional increase in the TCDD levels in line with the injected doses (STable 2, Suppl. Mat.).

The dose of 10 μg·kg^{-1} bw did not saturate the AT since higher concentrations of TCDD in the AT were obtained following the injection of 25 μg·kg^{-1} TCDD; thus, this dose (10 μg·kg^{-1} bw) was selected for all subsequent experiments (SFigure 1, Suppl Mat.).

The contaminated AT (epididymal left AT) were then grafted on uncontaminated host C57BL/6J mice. Fig. 2 shows that TCDD concentration decreases in the TCDD-contaminated grafted tissue in a time dependent manner.

3.2. TCDD redistributes to other tissues

Subsequently, we quantified the distribution of TCDD in three organs of the grafted mice, namely the epididymal AT of the host, liver and brain (respectively Fig. 3A and B, SFigure 2 Suppl. Mat). The levels of TCDD increased significantly in the host AT (Fig. 3A, from < 1 to > 100 pg·g^{-1} of fresh tissue in 3 weeks) during the 3-week-time period and remained then stable over the course of the experiments.

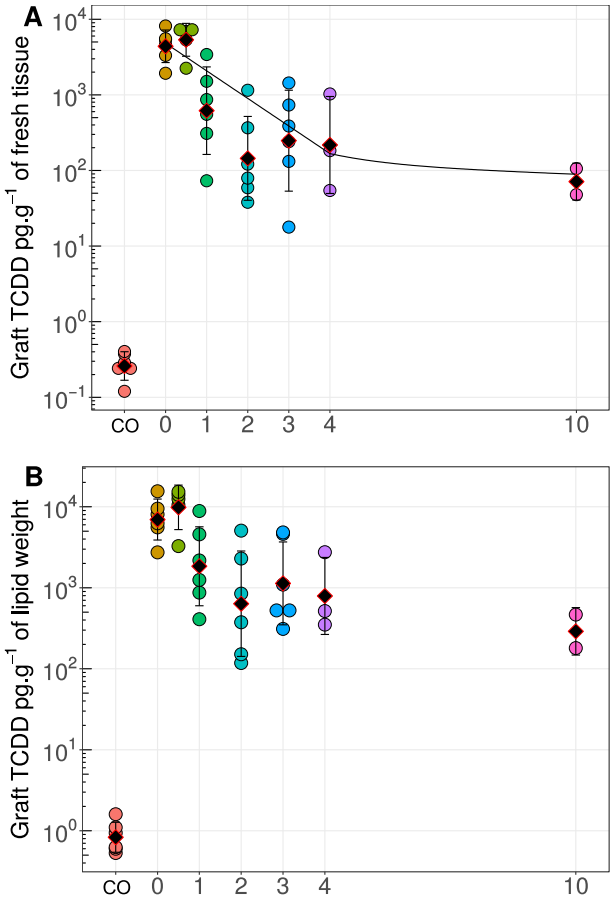

Fig. 2. Levels of TCDD (A: pg·g^{-1} fresh tissue; B: pg·g^{-1} lipid weight) measured in the grafted AT (3–6 mice/condition) at different time points following the graft (in weeks). The corn oil condition (CO) designates the level of TCDD present in a graft from mice injected with corn oil. In panel A, the line represents the profiled simulation of TCDD concentrations (expressed in pg TCDD·g^{-1} fresh tissue) from the graft implanted in dorsal subcutaneous for 10 weeks.

The distribution in the brain was slower than the distribution in the host AT, with a basal level of 0.1 pg·g^{-1} of fresh tissue and a concentration that reached 1 pg·g^{-1} of fresh tissue at 1 week and 10 pg·g^{-1} after 10 weeks (SFigure 2). The levels of TCDD also increased significantly in the liver (Fig. 3B, from < 0.1 to > 10 pg·g^{-1} of fresh tissue in 2 weeks) during the 2-week-time period and remained then stable over the course of the experiments.

When the levels of TCDD were represented in pg·g^{-1} of lipid weight (SFigure 3, Suppl. Mat.), a similar profile was obtained for the AT, a tissue with a high fat content. The fast and slow accumulations of TCDD respectively in the liver and the brain were also clearly characterized.

Overall, our experiments demonstrate that TCDD is quickly released from a contaminated grafted-AT and redistributed in several key organs of the grafted C57BL6 mice albeit with different kinetics.

3.3. PBPK modeling – exposure of the donor

The first step consisted to simulate the exposure of donor mice to a single intraperitoneal injection dose at concentrations of 1, 10 and 25 μg TCDD per kg bw (STable 2, Suppl. Mat.). Using the PBPK mouse model, we simulated the profile of TCDD concentrations in the AT (SFigure 4, Suppl. Mat.).

The simulation matched the experimental measurements of TCDD with very high accuracy (STable 2, Suppl. Mat. and SFigure 4, Suppl. Mat.) and the ratio of the nominal TCDD doses matched well with that

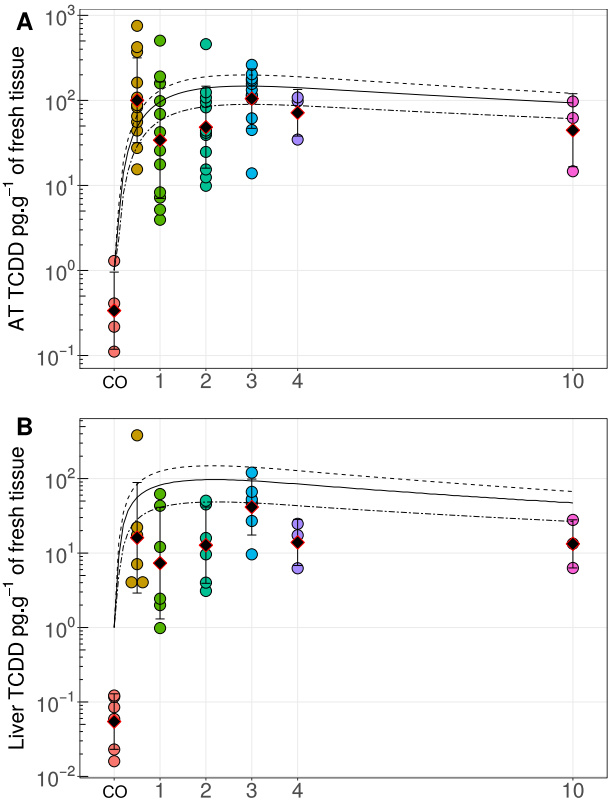

Fig. 3. Levels of TCDD (pg·g^{-1} of fresh tissue) in the host AT (A), and the liver (B) ($n = 6$ mice/condition except weeks 4 and 10) at different time points following the graft (in weeks). For all panels, the symbols (•) represent the individual measurement and the symbols (♦) represents the mean measurement and the standard deviation of the TCDD measured (mean ± SD) at different time points following the sacrifice. (A) simulation curves of the TCDD accumulation and experimental values in the AT and (B) in the liver issued from the host following subcutaneous grafting. For each of these tissues, we simulate the mean concentration at time 0, and the concentrations corresponding to the mean ± SD (see text). The corn oil condition (CO) designates the level of TCDD present in a graft from mice injected with corn oil.

of the measured TCDD concentrations in AT (Eq. (4)).

- **Equation 4**: Comparisons between ratio of dose and tissue concentrations:

$$\frac{\frac{10\mu g}{kg}}{1\mu g/kg} \cong \frac{\frac{21623pg}{gtissue}}{\frac{2335pg}{gtissue}} \cong 10 \quad \frac{\frac{25\mu g}{kg}}{\frac{1\mu g}{kg}} \cong \frac{\frac{56608pg}{gtissue}}{\frac{2335pg}{gtissue}} \cong 25 \tag{4}$$

3.4. PBPK modeling – release of TCDD from the graft/distribution of TCDD in host compartments

The second step consisted of simulating the decrease of TCDD in the graft. Because of the large standard deviations, we used the mean of TCDD concentrations measured in the different assays (4815 pg·g^{-1} fresh tissue at time 0). The first-order elimination rate constant was fixed at 0.004 h^{-1}. The concentration of TCDD in the graft was about 85 pg·g^{-1} fresh tissue at 10 weeks (corresponding to an elimination of 98.23%). The calculated half-life base based on the sequential point was 1.03 weeks on the first part of the biphasic curve (and 5.53 weeks for the second part of the curve).

We also simulated the accumulation of TCDD concentrations in the host AT and liver compartments following insertion of the graft. These compartments concentrate > 90% of the TCDD (Carrier, 1995). However, because the standard deviation (SD) of the initial concentration reflecting the amount of TCDD in the graft was relatively large, the simulation was performed using 1) the mean of the concentrations in the graft, 2) this mean + SD or 3) this mean – SD. Thus, for each compartment, 2 curves were simulated (Fig. 3). The prediction of the model was also accurate as the experimental data points for the liver and the AT were found between each maximal and minimal simulating curve (Fig. 3).

Overall, these two simulations (release and distribution) improved the confidence in the PBPK model for mice.

3.5. TCDD release from AT alters the expression of metabolic genes

We next investigated whether the TCDD released from graft-contaminated fat pad could alter expression of genes coding for TCDD-target genes, i.e. key biologic or disease-related functions. We and others have previously demonstrated that TCDD induced inflammation and fibrosis in the liver of exposed mice (Duval et al., 2017). Thus, we studied several biomarkers that could be related to chronic liver diseases (i.e. fibrosis, steatosis). We carried out RT-qPCR experiments using host liver and AT samples at 3 weeks after grafting.

We show that the levels of expression of AhR-target genes in the liver and AT were higher than at time 0, a result in line with a rapid contamination of these organs (Tables 3 and 4). In addition, the expression of fibrotic and inflammatory markers augmented also significantly, in line with our former studies on TCDD treated mice (Duval et al., 2017). The host AT also displayed an inflammatory profile (Table 4).

Due to the role of pyruvate carboxylase (PC), cytosolic phosphoenolpyruvate carboxykinase (PEPCK) and glucose 6 Phosphatase (G6Pase) in maintaining glycemia (potentially linked to type 2 diabetes), we investigated the expression of their genes in the liver and found that their mRNA content increased from time 0 to time 3-weeks following grafting.

4. Discussion

In the present study we provide direct experimental evidence for the release of TCDD from adipose tissue (AT, graft) and its migration into other tissues. We also show that the released pollutant induces relevant changes in gene expression in the target tissues and we characterize the kinetics of its distribution. The study was designed to address a knowledge gap and a methodological gap. Indeed, one of the most challenging issues in environmental toxicity is to understand and model long-term/low-dose effects (Barouki, 2010). Concerning POPs, such long-term effects are usually explained by continuous exposure due to

Table 3
Relative mRNA level of XME, inflammatory, fibrotic and metabolic marker in the liver following a 3-week internal exposure (statistically significant: $^{**}p < 0.01$, 6 animals per condition).

Function	Genes	Fold ind.
XME	AhR	2.65
	CYP1A1	8.96**
	CYP1B1	3.62**
Inflammation	IL-1ß	4.17**
	IL-6	1.25
	TNF alpha	1.94
	MCP-1	5.98**
	NOS2	2.42
	F4/80	3.42**
Fibrosis	COL1A1	3.93**
	Alpha-SMA	4.51**
Metabolism	Glycogen synthase 2	3.17**
	PC	3.01**
	Cytosolic PEPCK	2.94**
	G6Pase	2.39**
	PGC-1 alpha	2.24**

Table 4
Relative mRNA expression of several XME, inflammatory, fibrotic and metabolic markers in the AT following a 3-week internal exposure (statistically significant: *$p < 0.05$; **$p < 0.01$, 6 animals per condition).

Function	Genes	Fold ind.
XME	AhR	0.88
	CYP1A1	2.55*
	PAI-1	15.92*
Inflammation	IL-6	9.4**
	IL10	2.4
	TNF alpha	2.01*
	MCP-1	1.83*
	NOS2	1.35*
	CD68	2.79**
Metabolism	ATGL	1.67*
	HSL	0.66
	CPT1B	1.34
	VLCAD	2.10*
	AQP7	1.23
	CD36	0.49
	Cytosolic PEPCK	1.24*
	Glycerol Kinase	0.06*
	PDK4	3.82*
	PGC-1 alpha	1.18
	FABP4	3.93
	PPARα	0.85
	FAS	1.74
	UCP1	1.99*
	PPARg2	1.42

the persistence and bioaccumulation of those pollutants in the environment and by continuous release from internal storage sites such as the AT. It was not clear whether release from the AT was significant and whether it could induce biological or toxic effects in other tissues. Evidence for the latter mechanism has been gathered indirectly for example by studying weight loss in obese humans (Kim et al., 2011). The present study addresses specifically this point and provides direct evidence for the release of a POP from AT and describes its effects on other tissues. Thus, release of POPs from AT is likely to play a significant role in long-term effects of pollutants.

In order to study the release of POPs from the AT and its properties, we developed an adequate experimental model based on grafting of AT from a contaminated animal into a non-contaminated one. It explores the effects of a continuous release from an internal compartment, the AT and reflects exposures of humans and animals to POPs. Other models of continuous release do exist such as release capsules which have been designed mostly for pharmacological purposes (i.e. treatment of chronic pain) or micro-osmotic pumps (Mercadante, 2017; Tauer et al., 2013); however, both models differ from our model in the nature of the delivery compartment which is biologically relevant in our case and includes adipocytes, endothelial and immune cells which could influence the release. In that sense, the model described here is a better representation of the actual internal exposure than artificial models. However, it has its limitations too in that the graft could undergo different stresses and outcomes such a fibrosis or altered vascularization which may influence the observed results.

This AT graft model is clearly complementary to more traditional exposure models through ingestion or injection. It is not meant to be an alternative to other models but rather to identify the contributions of internal sources as compared to external exposures. In that sense it can help in assessing long-term effects even after withdrawal of external exposures. The model also allows the derivation of relevant toxicokinetic and toxicodynamic features that are complementary to those derived from classical drug treatment regimens.

Our experimental data improve the confidence in the PBPK model for mice that was developed previously (USEPA, 2012), and adapted for the present work. The intraperitoneal exposures to 1, 10 and 25 $\mu g \cdot kg^{-1}$ of body weight were also modeled (SFigure 4, Suppl. Mat.). The model accurately reproduces the experimental measurements, 48 h following the single intraperitoneal administration for all doses, regarding the ratio of doses and the amount measured in tissues (Eq. (1)). Yet, the model has its limitations since it requires surgery and some of the effects could be biased by the fate of the graft. Indeed, we observed individual differences in vascularization or fibrosis, which could impact TCDD release from the graft. These observations could partly explain why between 4 and 10 weeks, the slope of TCDD elimination from the graft, changes (Fig. 3); a better characterization of the vascularization of the graft will be necessary for our on-going projects. We believe that besides the structural variabilities described previously, metabolic adaptations and heterogeneous lipid content could also influence TCDD release. A better characterization of the graft would improve the description of the PBPK model. However, at this point, it predicts with accuracy the evolution of TCDD concentrations in both AT and liver known as the most important depository organs of this pollutant in mammals. Indeed, our experimental data that match the PBPK model, indicate that despite some variability in the initial concentrations of TCDD in the graft (mean of $4815 \pm 2122\ \mu g \cdot kg^{-1}$), the POP diffuses to other key organs such as the host AT, liver or brain following different kinetics. The release of TCDD from the graft is relatively rapid with a half-life of 1.03 weeks (≅173 h, from weeks 0–4) and 5.53 weeks (932 h from week 4), suggesting that after 10 weeks, > 97% has been released from the graft. The modeled kinetics of release and distribution is in line with the experimental data (Fig. 3); this simulation represents an exciting predictive tool which also could be improved in the future using a wider range of POPs and representative mixtures.

The release of TCDD influences important biological pathways that are involved in liver and AT dysfunction. For this part of the work, the focus was first on xenobiotic metabolizing enzymes (biomarkers of an activated AhR signaling pathway) and inflammatory cytokines/chemokines which are classically induced upon TCDD exposure. As expected (regarding the distribution of TCDD), the AhR-target genes (CYP1A1, CYP1B1, PAI-1) were significantly induced at the mRNA levels in the liver and AT 3 weeks following grafting (Tables 3 and 4). Similarly, an inflammatory signature is observed in both tissues which is in line with the literature and our former studies using traditional modes of exposure (Duval et al., 2017; Kim et al., 2011, 2012). Furthermore, a highly significant increase of the expression of two biomarkers of fibrosis in the liver (alpha-Smooth Muscle Action or alpha-SMA and collagen 1A1 or COL1A1IL) was obtained, confirming our recent observations on the occurrence of liver fibrosis following exposure to TCDD (Duval et al., 2017). Finally, the mRNA expression of the three key gluconeogenic enzymes, pyruvate carboxylase (PC), cytosolic phosphoenolpyruvate carboxykinase (PEPCK), glucose 6-phosphatase (G6Pase) showed significant inductions. Such enzymes contribute to the maintenance of glycemia during fasting, but their induction is also classically described in type 2 diabetes (Beale et al., 2007). These results are different from those of other teams who reported that expression of PEPCK is strongly repressed by TCDD; in 1993, Stahl et al. demonstrated that TCDD exposure decreased hepatic gluconeogenesis due to a reduction of PEPCK activity and mRNA expression (Stahl et al., 1993) which has been also observed in another model by Dunlap et al. (2002). This was also demonstrated for PC following a short treatment in hepatic rat livers (Ilian et al., 1996). We hypothesize that the difference between those observations and our data is due to the mode of exposure; most previous experiments were performed using an acute-based exposure protocol while our model allows a constant delivery of TCDD for several weeks. While we are not able at this point to explain mechanistically the differences, we think that a sustained low-dose delivery of TCDD could have a different impact than an acute delivery of TCDD, on the regulation of gluconeogenesis enzymes.

This observation suggests that a continuous exposure of TCDD could disrupt carbohydrate and lipid metabolism and, more generally, liver functions. Thus, the TCDD released from an internal storage site can

induce gene expression changes in at least two tissues that reflect biological activity of this pollutant and which is in line with what is known about its toxicity. While it is likely that some of the effects of TCDD on gene expression are related to the activation of the AhR pathway (such as the induction of CYP1 genes), other effects may be indirect. For example, TCDD and the AhR activate the expression of inflammatory cytokines through direct or indirect, genomic or non-genomic pathways (Kim et al., 2012), and those cytokines could also be responsible for the other genomic alterations observed in the liver and the AT; moreover, as the release of TCDD from the graft is relatively rapid and then high, these gene expressions could represent an adaptive response to a major environmental stress (a high dose of TCDD). In order to delineate the actual mechanisms involved in the effects of contaminated/xenografted-AT on gene expression in distant tissues after such periods of exposure (3 weeks in our case), additional studies would be required. Thus, we can conclude that the release of POPs from internal storage sites could play a significant role in the toxicity of those pollutants that needs to be further investigated using a wider range of POPs and representative mixtures.

5. Conclusion

The experimental model described here represents a novel approach to explore exposure to pollutants from endogenous sources and their long-term toxicities. It is meant to be complementary to other experimental protocols of exposure through diet, dermal, intraperitoneal injection or gavage procedures.

Acknowledgments and funding

This work was supported by the ANSES (N°EST-2012/2/156) (ALLOFATOX-Funding including PhD fellowship: N. Joffin), the Université Paris Descartes-COMUE-SPC (Funding), INSERM (Funding), Assistance Publique-Hôpitaux-de-Paris, the LUNAM Université (Funding).

A competing financial interest's declaration

All authors have disclosed that there is no actual or potential competing interest regarding the submitted article.

Appendix A. Supplementary data

Supplementary data to this article can be found online at https://doi.org/10.1016/j.envint.2018.10.027.

References

Ambolet-Camoit, A., Ottolenghi, C., Leblanc, A., Kim, M.-J., Letourneur, F., Jacques, S., Cagnard, N., Guguen-Guillouzo, C., Barouki, R., Aggerbeck, M., 2015. Two persistent organic pollutants which act through different xenosensors (alpha-endosulfan and 2,3,7,8 tetrachlorodibenzo-p-dioxin) interact in a mixture and downregulate multiple genes involved in human hepatocyte lipid and glucose metabolism. Biochimie 116, 79–91.

Barouki, R., 2010. Linking long-term toxicity of xeno-chemicals with short-term biological adaptation. Biochimie 92, 1222–1226. https://doi.org/10.1016/j.biochi.2010.02.026.

Beale, E.G., Harvey, B.J., Forest, C., 2007. PCK1 and PCK2 as candidate diabetes and obesity genes. Cell Biochem. Biophys. 48, 89–95.

Boffetta, P., Mundt, K.A., Adami, H.-O., Cole, P., Mandel, J.S., 2011. TCDD and cancer: a critical review of epidemiologic studies. Crit. Rev. Toxicol. 41 (7), 622–636.

Bonde, J.S., Flachs, E.M., Rimborg, S., Glazer, C.H., Giwercman, A., 2016. The epidemiologic evidence linking prenatal and postnatal exposure to endocrine disrupting chemicals with male reproductive disorders: a systematic review and meta-analysis. Hum. Reprod. Update 23, 104–125.

Brown, R.P., Delp, M.D., Lindstedt, S.L., Rhomberg, L.R., Beliles, R.P., 1997. Physiological parameter values for physiologically based pharmacokinetic models. Toxicol. Ind. Health 13, 407–484. https://doi.org/10.1177/074823379701300401.

Carrier, G., 1995. Modeling of the Toxicokinetics of polychlorinated dibenzo-p-dioxins and dibenzofurans in mammalians, including humans I. Nonlinear distribution of PCDD/PCDF body burden between liver and adipose tissues. Toxicol. Appl. Pharmacol. 131, 253–266. https://doi.org/10.1006/taap.1995.1068.

Chevrier, J., Dewailly, E., Ayotte, P., Mauriège, P., Després, J.P., Tremblay, A., 2000. Body weight loss increases plasma and adipose tissue concentrations of potentially toxic pollutants in obese individuals. Int. J. Obes. Relat. Metab. Disord. 24 (10), 1272–1278.

Costera, A., Feidt, C., Marchand, P., Le Bizec, B., Rychen, G., 2006. PCDD/F and PCB transfer to milk in goats exposed to a long-term intake of contaminated hay. Chemosphere 64 (4), 650–657.

Diliberto, J.J., Burgin, D., Birnbaum, L.S., 1997. Role of CYP1A2 in hepatic sequestration of dioxin: studies using CYP1A2 knock-out mice. Biochem. Biophys. Res. Commun. 236, 431–433. https://doi.org/10.1006/bbrc.1997.6973.

Dunlap, D.Y., Ikeda, I., Nagashima, H., Vogel, C.F., Matsumura, F., 2002. Effects of src-deficiency on the expression of in vivo toxicity of TCDD in a strain of c-src knockout mice procured through six generations of backcrossings to C57BL/6 mice. Toxicology 172, 125–141.

Duval, C., Teixeira-Clerc, F., Leblanc, A.F., Touch, S., Emond, C., Guerre-Millo, M., Lotersztajn, S., Barouki, R., Aggerbeck, M., Coumoul, X., 2017. Chronic exposure to low doses of dioxin promotes liver fibrosis development in the C57BL/6J diet-induced obesity mouse model. Environ. Health Perspect. 125, 428–436.

Emond, C., 2004. Physiologically based pharmacokinetic model for developmental exposures to TCDD in the rat. Toxicol. Sci. 80, 115–133. https://doi.org/10.1093/toxsci/kfh117.

Emond, C., Michalek, J.E., Birnbaum, L.S., DeVito, M.J., 2005. Comparison of the use of a physiologically based pharmacokinetic model and a classical pharmacokinetic model for dioxin exposure assessments. Environ. Health Perspect. 113, 1666–1668.

Emond, C., Birnbaum, L.S., DeVito, M.J., 2006. Use of a physiologically based pharmacokinetic model for rats to study the influence of body fat mass and induction of CYP1A2 on the pharmacokinetics of TCDD. Environ. Health Perspect. 114, 1394–1400.

Emond, C., Raymer, J.H., Studabaker, W.B., Garner, C.E., Birnbaum, L.S., 2010. A physiologically based pharmacokinetic model for developmental exposure to BDE-47 in rats. Toxicol. Appl. Pharmacol. 242, 290–298.

Emond, C., DeVito, M., Warner, M., Eskenazi, B., Mocarelli, P., Birnbaum, L.S., 2016. An assessment of dioxin exposure across gestation and lactation using a PBPK model and new data from Seveso. Environ. Int. 92-93, 23–32.

Emond, C., DeVito, M.J., Diliberto, J.J., Birnbaum, L.S., 2018. The influence of obesity on the pharmacokinetics of dioxin in mice: an assessment using classical and PBPK modeling. Toxicol. Sci. https://doi.org/10.1093/toxsci/kfy078.

Goodman, M., Narayan, K.M.V., Flanders, D., Chang, E.T., Adami, H.-O., Boffetta, P., Mandel, J.S., 2015. Dose-response relationship between serum 2,3,7,8-tetrachlorodibenzo-p-dioxin and diabetes mellitus: a meta-analysis. Am. J. Epidemiol. 181 (6), 374.

Guyot, E., Chevallier, A., Barouki, R., Coumoul, X., 2013. The AhR twist: ligand-dependent AhR signaling and pharmaco-toxicological implications. Drug Discov. Today 18, 479–486.

Ilian, M.A., Sparrow, B.R., Ryu, B.W., Selivonchick, D.P., Schaup, H.W., 1996. Expression of hepatic pyruvate carboxylase mRNA in C57BL/6J Ah(b/b) and congenic Ah((d/d)) mice exposed to 2,3,7,8-tetrachlorodibenzo-p-dioxin. J. Biochem. Toxicol. 11, 51–56.

Imbeault, P., Chevrier, J., Dewailly, E., Ayotte, P., Després, J.P., Mauriège, P., Tremblay, A., 2002. Increase in plasma pollutant levels in response to weight loss is associated with the reduction of fasting insulin levels in men but not in women. Metabolism 51 (4), 482–486.

Juricek, L., Bui, L.-C., Busi, F., Pierre, S., Guyot, E., Lamouri, A., Dupret, J.-M., Barouki, R., Coumoul, X., Rodrigues-Lima, F., 2014. Activation of the aryl hydrocarbon receptor by carcinogenic aromatic amines and modulatory effects of their N-acetylated metabolites. Arch. Toxicol. https://doi.org/10.1007/s00204-014-1367-7.

Kim, M.-J., Marchand, P., Henegar, C., Antignac, J.-P., Alili, R., Poitou, C., Bouillot, J.-L., Basdevant, A., Le Bizec, B., Barouki, R., Clément, K., 2011. Fate and complex pathogenic effects of dioxins and polychlorinated biphenyls in obese subjects before and after drastic weight loss. Environ. Health Perspect. 119, 377–383. https://doi.org/10.1289/ehp.1002848.

Kim, M.-J., Pelloux, V., Guyot, E., Tordjman, J., Bui, L.-C., Chevallier, A., Forest, C., Benelli, C., Clément, K., Barouki, R., 2012. Inflammatory pathway genes belong to major targets of persistent organic pollutants in adipose cells. Environ. Health Perspect. 120, 508–514.

Kissel, J.C., Robarge, G.M., 1998. Assessing the elimination of 2,3,7,8-TCDD from humans with a physiologically based pharmacokinetic model. Chemosphere 17, 2017–2027. https://doi.org/10.1016/0045-6535(88)90012-4.

La Merrill, M., Emond, C., Kim, M.-J., Antignac, J.-P., Le Bizec, B., Clement, K., Birnbaum, L.S., Barouki, R., 2013. Toxicological function of adipose tissue: focus on persistent organic pollutants. Environ. Health Perspect. 121, 162–169.

Lee, Y.M., Kim, K.S., Jacobs, D.R., Lee, D.H., 2017. Persistent organic pollutants in adipose tissue should be considered in obesity research. Obes. Rev. 18 (2), 129–139.

Lee, Y.-M., Kim, S.-A, Lee, I.-K., Kim, J.-G., Park, K.-G., Jeong, J.-Y., Jeon, J.-H., Shin, J.-Y., Lee, D.-H., 2016. Effect of a Brown Rice Based Vegan Diet and Conventional Diabetic Diet on Glycemic Control of Patients with Type 2 Diabetes: A 12-Week Randomized Clinical Trial. PLoS One 11 (6), e0155918.

Leung, H., Ku, R.H., Paustenbach, D.J., Andersen, M.E., 1988. A physiologically based pharmacokinetic model for 2,3,7,8-tetrachlorodibenzo-p-dioxin in C57BL/6J and DBA/2J mice. Toxicol. Lett. 42, 15–28.

Leung, H., Paustenbach, D.J., Murray, F., Andersen, M.E., 1990. A physiological pharmacokinetic description of the tissue distribution and enzyme-inducing properties of 2,3,7,8-tetrachlorodibenzo-p-dioxin in the rat. Toxicol. Appl. Pharmacol. 103, 399–410.

Mercadante, S., 2017. Oxycodone extended release capsules for the treatment of chronic pain. Expert. Rev. Neurother. 17, 427–431.

Mostafalou, S., 2016. Persistent organic pollutants and concern over the link with insulin resistance related metabolic diseases. Rev. Environ. Contam. Toxicol. 238, 69–89.
Novelli, M., Piaggi, S., De Tata, V., 2005. 2,3,7,8-Tetrachlorodibenzo-p-dioxin-induced impairment of glucose-stimulated insulin secretion in isolated rat pancreatic islets. Toxicol. Lett. 156 (2), 307–314.
Pfaffl, M.W., 2001. A new mathematical model for relative quantification in real-time RT-PCR. Nucleic Acids Res. 29, e45.
Smarr, M.M., Kannan, K., Buck Louis, G.M., 2016. Endocrine disrupting chemicals and endometriosis. Fertil. Steril. 106 (4), 959–966.
Stahl, B.U., Beer, D.G., Weber, L.W., Rozman, K., 1993. Reduction of hepatic phosphoenolpyruvate carboxykinase (PEPCK) activity by 2,3,7,8-tetrachlorodibenzo-p-dioxin (TCDD) is due to decreased mRNA levels. Toxicology 79, 81–95.
Tauer, J.T., Hofbauer, L.C., Jung, R., Erben, R.G., Suttorp, M., 2013. Micro-osmotic pumps for continuous release of the tyrosine kinase inhibitor bosutinib in juvenile rats and its impact on bone growth. Med. Sci. Monit. Basic Res. 19, 274–278.
USEPA, 2012. EPA's Reanalysis of Key Issues Related to Dioxin Toxicity and Response to NAS Comments. (EPA/600/R-10/038F).
Wang, X., Santostefano, M.J., Evans, M.V., Richardson, V.M., Diliberto, J.J., Birnbaum, L.S., 1997. Determination of parameters responsible for pharmacokinetic behavior of TCDD in female Sprague–Dawley rats. Toxicol. Appl. Pharmacol. 147, 151–168. https://doi.org/10.1006/taap.1997.8242.
White, S.S., Birnbaum, L.S., 2009. An overview of the effects of dioxins and dioxin-like compounds on vertebrates, as documented in human and ecological epidemiology. J. Environ. Sci. Health C Environ. Carcinog. Ecotoxicol. Rev. 27, 197–211. https://doi.org/10.1080/10590500903310047.